JCIM JOURNAL OF CHEMICAL INFORMATION AND MODELING

pubs.acs.org/jcim Article

Discovery of Nanomolar Inhibitors for Human Dihydroorotate Dehydrogenase Using Structure-Based Drug Discovery Methods

William T. Higgins, Sandip Vibhute, Chad Bennett, and Steffen Lindert*

Cite This: J. Chem. Inf. Model. 2024, 64, 435−448 Read Online

ACCESS | Metrics & More | Article Recommendations | Supporting Information

ABSTRACT: We used a structure-based drug discovery approach to identify novel inhibitors of human dihydroorotate dehydrogenase (DHODH), which is a therapeutic target for treating cancer and autoimmune and inflammatory diseases. In the case of acute myeloid leukemia, no previously discovered DHODH inhibitors have yet succeeded in this clinical application. Thus, there remains a strong need for new inhibitors that could be used as alternatives to the current standard-of-care. Our goal was to identify novel inhibitors of DHODH. We implemented prefiltering steps to omit PAINS and Lipinski violators at the earliest stages of this project. This enriched compounds in the data set that had a higher potential of favorable oral druggability. Guided by Glide SP docking scores, we found 20 structurally unique compounds from the ChemBridge EXPRESS-pick library that inhibited DHODH with $IC_{50,\ DHODH}$ values between 91 nM and 2.7 μM. Ten of these compounds reduced MOLM-13 cell viability with $IC_{50,\ MOLM\text{-}13}$ values between 2.3 and 50.6 μM. Compound **16** ($IC_{50,\ DHODH}$ = 91 nM) inhibited DHODH more potently than the known DHODH inhibitor, teriflunomide ($IC_{50,\ DHODH}$ = 130 nM), during biochemical characterizations and presented a promising scaffold for future hit-to-lead optimization efforts. Compound **17** ($IC_{50,\ MOLM\text{-}13}$ = 2.3 μM) was most successful at reducing survival in MOLM-13 cell lines compared with our other hits. The discovered compounds represent excellent starting points for the development and optimization of novel DHODH inhibitors.

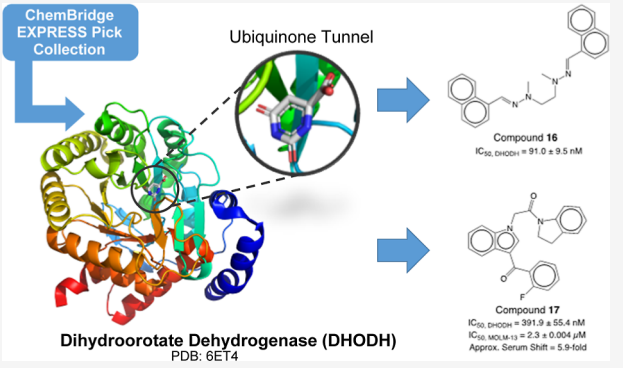

INTRODUCTION

Acute myeloid leukemia (AML) is a devastating cancer that can affect any age group, but the highest incidence occurs in people over the age of 65. Despite prognostic improvements made over the past 30 years, more than half of young adult patients and approximately 90% of elderly patients still die from this disease.[1] In healthy patients, myeloid cells transition from self-renewing progenitor cells to terminally differentiated cells with lower proliferation rates, to limit the lifespan of the cell. A hallmark of AML is the disruption of this normal maturation process that causes leukemic cells to arrest at the proliferative undifferentiated stage.[2] This differentiation blockade culminates in a variety of mutational events, making AML a highly heterogeneous disease.[3] A combination of treatment paradigms is necessary in almost all of the AML cases. Even with aggressive approaches that involve cytotoxic chemotherapy, achieving durable remissions is notoriously a challenge.[4] The efficacy of existing treatments ranges depending on age; 35−40% cure is typically obtained for AML patients younger than 60 years of age, but this falls to only 5−15% in adults over the age of 60.[5] Thus, there is a need for new therapeutic avenues with novel mechanisms of action from what is currently used as the standard-of-care.

Previous work by Sykes and colleagues identified dihydroorotate dehydrogenase (DHODH) as an attractive therapeutic target because small molecule inhibition of this enzyme can overcome the differentiation blockade in AML.[6,7] In humans, class 2 DHODH is a ubiquitous, flavin-dependent enzyme localized to the inner membrane of the mitochondria.[6,8] DHODH catalyzes the oxidation of L-dihydroorotate (DHO) to orotate (ORO), which is the rate-limiting step in *de novo* biosynthesis of uridine monophosphate (UMP).[9] Pyrimidine starvation induced through DHODH inhibition arrests the cell cycle at the S-phase, where nucleotides must be readily available for continued growth.[10] DHODH inhibition also has a direct effect on mRNA translation by perturbing ribosome biogenesis. Ribosynthesis, specifically, is one of the most energetically demanding processes orchestrated within the cell and relies on a steady source of nucleotides to successfully complete. Thus, ribosomal stress through pyrimidine starvation causes cell cycle arrest and the inevitable apoptosis of tumor cells. This is not a ubiquitous effect across different cell types,

Received: August 24, 2023
Revised: December 21, 2023
Accepted: December 21, 2023
Published: January 4, 2024

https://doi.org/10.1021/acs.jcim.3c01358
J. Chem. Inf. Model. 2024, 64, 435−448

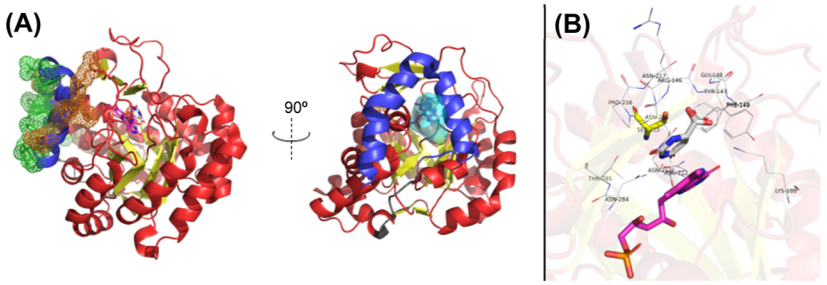

Figure 1. Cartoon illustration of human DHODH. (A) N-terminal domain responsible for transmembrane association is colored with blue ribbons. The C-terminal domain is shown with red ribbons with the $(\alpha\beta)_8$ barrel colored yellow. A hydrophobic protrusion that pushes into the inner mitochondrial membrane is shown with a green mesh, and the orange mesh illustrates positively charged residues on the periphery of this protrusion that interact with the polar head groups of the phospholipid bilayer. The cyan surface illustrates the inhibitor binding site at the interface between the N- and C-domains. (B) DHO (gray sticks) and FMN (magenta sticks) occupy a site above the $(\alpha\beta)_8$ barrel and distal to the inhibitor binding site. Residues within a 4.0 Å radius of DHO are displayed, with the catalytic serine colored with yellow sticks.

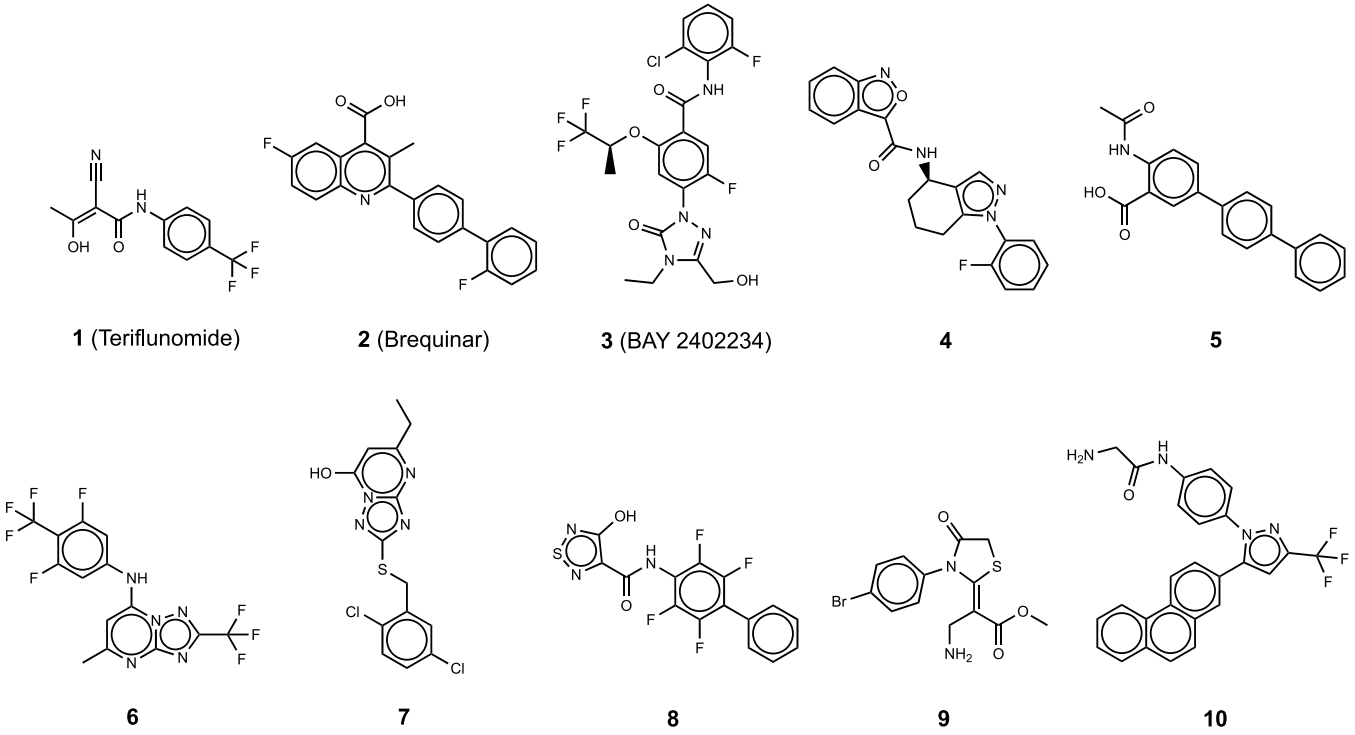

Figure 2. Structures of cocrystallized DHODH inhibitors used in self-docking simulations. Compounds **1**−**10** correspond to the bound inhibitors in 1D3H, 1UUO, 6QU7, 6ET4, 2WV8, 4OQV, 3ZWT, 5MVC, 5H2Z, and 6OC0, respectively.

particularly for healthy cells, which can engage in alternative strategies to acquire nucleotides.[11] On the one hand, nonleukemia cells compensate for uridine deficiency by turning to exogenous uridine to drive cellular proliferation.[12] On the other hand, cancer cells, including AML types, have altered metabolic states and increased proliferation rates that makes their capacity to self-renew sensitive to pyrimidine starvation.[13] The result is selection of differentiation over proliferation, which has been demonstrated in multiple AML models.[12,14]

The structure of class 2 DHODH is characterized by two domains in higher order eukaryotes (Figure 1A). The N-terminal domain contains two α-helices and a transmembrane sequence that anchors DHODH to the inner mitochondrial membrane by a hydrophobic protrusion and positively charged periphery, and the C-terminal domain houses a large $(\alpha\beta)_8$ barrel.[8,9,15,16] The active site of DHODH is found above the $(\alpha\beta)_8$ barrel and displays a serine residue in close contact with DHO as the catalytic base for the stereospecific oxidation to the ORO (Figure 1B). The binding site for the cofactors flavin mononucleotide (FMN) and ubiquinone is located proximal to the $(\alpha\beta)_8$ barrel at the interface between the active site and the N-terminal domain. Small molecule inhibitors competitively abrogate DHODH activity by displacing DHO or ubiquinone from their respective binding sites. This lowers the intracellular pools of uracil, cytosine, and thymidine nucleotides, which healthy cells can compensate for by turning to the salvage pathway.[9,15]

Numerous DHODH inhibitors have been reported over the years for the purposes of treating cancer, autoimmune, and inflammatory diseases, but very few have actually progressed to human trials.[8,15,17−19] Leflunomide, teriflunomide (the active metabolite of leflunomide; compound **1**, Figure 2), and brequinar (compound **2**, Figure 2) are among the most well-known DHODH inhibitors. Even though these drugs do achieve pyrimidine depletion mediated by DHODH inhibition, adverse side effects have remained persistent that limit their

https://doi.org/10.1021/acs.jcim.3c01358
J. Chem. Inf. Model. 2024, 64, 435−448

therapeutic applications. Compound **2** and its analogs are immunosuppressants that have previously advanced to stage I clinical studies in the 1990s with a focus on patients with solid tumors, but not myeloid malignancies.[3] Indeed, there was some success when compound **2** and its analogs were combined synergistically with cyclosporine or cisplatin, but daily administration resulted in a toxic accumulation of the drug that limited clinical use.[15,20,21] Leflunomide and its active metabolite, compound **1**, are FDA-approved drugs for treating rheumatoid arthritis and multiple sclerosis, respectively. The serendipitous utility of these drugs in regards to antitumor efficacy was initially promising, but both drugs have been linked to hepatotoxicity and interstitial lung disease.[15,22] Furthermore, leflunomide and compound **1** have exhibited specificity for alternative targets, as well. This opens the possibility that the antitumor effects of these drugs, at least to some degree, are not facilitated through DHODH inhibition alone.[3] More recently, BAY 2402234 (compound **3**, Figure 2) has emerged as a potent and highly specific inhibitor of DHODH. Compound **3** has demonstrated promising therapeutic potential both in vitro and in vivo. However, compound **3** has also been noted to induce a downregulation in genes that encode for critical components in adult hematopoiesis and *N*-acetyl glycosylation metabolism.[3] In summary, the astonishingly low number of efficacious anticancer DHODH inhibitors warrants further investigation and discovery of new small molecule leads.

The drug discovery timeline involves four general stages: target characterization, lead optimization, bioavailability studies, and clinical trials.[23] Despite encouraging preclinical data, previously identified DHODH inhibitors have not yet demonstrated significant efficacy in cancer clinical trials.[24] Nonetheless, we remain optimistic about DHODH as a cancer target and strive to discover novel inhibitors that will not exhibit similar limitations. We selected compounds with favorable properties for oral druggability by eliminating PAINS and Lipinski violators at the earliest stages of this study. Additionally, the ChemBridge EXPRESS-pick collection has been curated to survey a broad chemical space representative of drug-like and lead-like compounds that could be further optimized at later stages in the drug discovery pipeline. We used structure-based drug discovery (SBDD), a well-established and successful technique to identify new leads for a protein of interest. Screening large numbers of compounds in a laboratory-based setting is an expensive, time-consuming, and labor-intensive task. The use of virtual screening methodologies to expedite the drug development timeline have gained momentum over recent years by substantially reducing the number of ligands that will need to be validated through experimental assays.[25] Previously, our group and others have successfully implemented SBDD to identify small molecule binders for infectious and neurodegenerative diseases, cancer, heart failure, and various other acute conditions.[12,15,24−50]

In this work, we present an SBDD approach to computationally model ligand interactions with DHODH and identify novel inhibitors of this enzyme. We effectively used a high-throughput virtual screening approach to evaluate 461,106 small molecules from the ChemBridge EXPRESS-pick library. This project was geared toward finding compounds that would have favorable oral druggability and could be used as starting points for further lead optimization. We identified the best inhibitor candidates in silico based on docking score and ligand efficiency. We experimentally validated these compounds in vitro, and 20 compounds demonstrated potential to act as DHODH inhibitors judged by an enzymatic activity assay to measure the biochemical IC_{50}. We further characterized these 20 compounds with a cellular viability assay in MOLM-13 cells to assess possible serum shift effects. From this, we identified 10 novel DHODH inhibitors with biochemical and cellular IC_{50} values as low as 91 nM and 2.3 μM, respectively.

METHODS

DHODH Structure Collation and Selection. We conducted a search within the RCSB Protein Data Bank (PDB)[51] for deposited structures of human class 2 DHODH. From this search, we selected accession codes 1UUO, 2WV8, 3ZWT, 4OQV, 5H2Z, 1D3H, 5MVC, 6ET4, 6OC0, and 6QU7 based on a crystallographic resolution of approximately 2.0 Å or better and the presence of a cocrystallized inhibitor (Figure 2). 1UUO is a structure for rat DHODH, but this remained in our initial selection because it is representative of human class 2 DHODH structures and contains well-established compound **2**. All of the selected DHODH structures were derived using X-ray crystallography.

Protein and Ligand Preparation. All DHODH structures selected for this study were imported into Maestro by Schrödinger and prepared using the Protein Preparation Wizard.[52] EPIK was used to assign protonation states of all ionizable residues within a pH range of 7.4 ± 1.0.[53] All nonprotein atoms were removed from each prepared structure, with the exception of FMN and the natural ligand, ORO. FMN and the ORO provide a structural role in the active site of DHODH, so keeping those in the structure was more representative of benchtop conditions. We used the LigPrep module of the Schrödinger suite to prepare each ligand for docking. This also used EPIK to assign ligand protonation states at a pH value of 7.4 ± 1.0.[53] LigPrep was configured to exhaustively generate all possible tautomers and stereoisomers for every input molecule.[54] The coordinates of each cocrystallized inhibitor were extracted from their respective PDBs. All other possible inhibitors that were evaluated in this study came from existing SDF files that provided three-dimensional structural information for each molecule.

Molecular Docking Methodology. The cocrystallized inhibitors from PDB IDs 1UUO, 2WV8, 3ZWT, 4OQV, 5H2Z, 1D3H, 5MVC, 6ET4, 6OC0, and 6QU7 were extracted and docked back into their respective receptor conformations using Schrödinger's Glide[55] standard precision (SP) scoring function. We used this self-docking approach to determine which DHODH conformations performed best at reproducing experimentally determined inhibitor poses during docking. Performance was assessed by the calculation of the in-place root-mean-square deviation (rmsd) of the lowest scoring docked pose to the experimental position. The lower the in-place rmsd, the higher we considered the predictive accuracy to be for a model. Following previously established protocols,[56] we used an in-place rmsd cutoff of 2.0 Å or lower to define success in our self-docking simulations.

We chose to use Glide SP to perform molecular docking in this study. Glide SP uses a series of hierarchical filters to exhaustively sample the conformational, orientational, and positional landscape for each ligand.[55,57] The docked pose was deterministically returned after a final geometry optimization was performed using the OPLS3e force field. We defined the search space as a receptor grid in each DHODH structure

https://doi.org/10.1021/acs.jcim.3c01358
J. Chem. Inf. Model. 2024, 64, 435−448

where Glide SP would determine the final docking poses. Receptor grids were generated by selecting the cocrystallized inhibitor in the Maestro workspace for each protein structure. We used the center of the molecule to define the center of the receptor grid box. This allowed the centroids of any docked molecules to sample a 10 × 10 × 10 Å inner search space, while the periphery of each molecule could extend 20 Å in any direction.[58] Any residues that could freely rotate within the receptor grid were allowed to do so. We opted to use flexible ligand sampling to consider the effects of stereoisomers, alternative ring conformers, or pyramidal nitrogen inversions when these options were possible. In-place rmsds were calculated by comparing the positions of all heavy atoms in the docked pose to the input coordinates without superimposition.

Virtual Screening and Prefiltering. We used the EXPRESS-Pick Collection from ChemBridge Corporation (San Diego, CA, USA) for virtual screening. The EXPRESS stock contains 502,530 diverse small molecules that represent drug- and lead-like compounds. Since our goal was to identify new chemotypes for therapeutic application through DHODH inhibition, we implemented prescreening steps to augment the efficiency of our virtual screening efforts. These prescreening steps excluded any compounds with functional groups implicated as pan-assay interference compounds (PAINS) and those which contained more than one violation of Lipinski's Rule of Five.[59,60] We executed these prescreening steps using the 2021.09.5 release of the RDKit package in Python 3.9.[61] The prefiltering steps were carried out by converting every ligand in the EXPRESS library from the SDF format to an RDKit molecule object. This process removed 40,036 molecules that qualified as either PAINS compounds or Lipinski violators. A total of 462,494 ligands remained after prefiltering. A final check was done to remove any duplicate entries that resulted in an additional 1388 molecules being removed.

The remaining 461,106 ligands were docked into 6ET4 using Glide SP with the default settings. The same receptor grid that was employed during self-docking with 6ET4 was also used for virtual screening purposes. As a basis for comparison, known active DHODH inhibitors were queried from the ChEMBL database and also docked into the 6ET4 receptor grid following the removal of PAINS and Lipinski violators. Ligands docked from the EXPRESS library were ranked by docking score and ligand efficiency to obtain two distinct lists of compounds that were considered for experimental validation. Only the top scoring pose of each conformer was retained in these lists to avoid duplicate entries. We refined the top in silico hits in these lists based on our chemical intuition. Some entries contained in the ligand efficiency list were exceptionally small or existed as a salt. At this early stage of the drug discovery process, we deliberately excluded salts to better investigate the exact chemical species responsible for any observations during the experimental validation steps. Additionally, this change also added uniformity in solubility, considering that salts have different solubility properties compared to their neutral forms. This was addressed by excluding molecules with a MW less than 130 g/mol or those that would need to be ordered as a salt. This condition was also applied to the list ranked by docking score, but it did not result in the removal of any additional molecules.

The results of virtual screening and additional refinement by our chemical intuition were two lists ranked by docking score (EXPRESS Library "group 1") and ligand efficiency (EXPRESS Library "group 2") and consisted of 79 and 97 compounds each, respectively. Ligand efficiency is the quotient of the docking score and the number of heavy atoms in the ligand, which allows for a quantitative comparison of hits that is dependent on the molecular weight. We verified that the ligands contained within these lists were structurally unique from one another by calculating pairwise Tanimoto indices. In addition, we also calculated Tanimoto indices between these compounds and compounds **1**−**10** to assess similarity to some known DHODH inhibitors. We used a cutoff value of ≥0.65 to mark compounds that should be considered structurally similar.

Expression and Purification. Recombinant human DHODH (residues 31−395; Uniprot Q02127) was prepared by Reaction Biology Corp. (Malvern, PA, USA). The protein was expressed with an N-terminal His_8-SUMO tag and a C-terminal StrepII tag in *Escherichia coli*. Rosetta 2 cells were induced with 0.25 mM IPTG and incubated in TB at 18 °C overnight. Transformed cells were lysed in a buffer containing 50 mM HEPES (pH 8.0), 500 mM NaCl, 10% glycerol, 5 mM $MgCl_2$, 0.25 mM TCEP, 0.25 mM ORO, 0.1 mM FMN, and a benzamidine protease inhibitor cocktail. Protein purification involved Strep-Tactin Superflow Agarose (IBA) resin with on-column ULP protease cleavage to remove the SUMO tag prior to elution in buffer containing 2.5 mM desthiobiotin. The protein was further purified using Superdex 75 (GE Healthcare) size exclusion chromatography. The final formulation buffer consisted of 50 mM HEPES (pH 8.0), 400 mM NaCl, 5% glycerol, 0.25 mM ORO, 1 mM EDTA, and 0.25 mM TCEP.

Enzyme Activity Assay. 176 ligands were obtained from ChemBridge in total, 79 and 97 from the lists ranked by either docking score (EXPRESS Library "group 1") or ligand efficiency (EXPRESS Library "group 2"), respectively, in 10 mM DMSO. Compound purity was confirmed by quantitative H^1 NMR and LCMS. All compounds were tested against human DHODH by Reaction Biology Corporation (Malvern, PA, USA). A fluorescence-based enzymatic activity assay was conducted in aqueous buffer at pH 7.0 containing reaction buffer (100 mM HEPES, 150 mM NaCl, 0.3% CHAPS, 0.5 mg/mL BSA, 0.1 μM FMN, and 1% DMSO), 5 nM DHODH, 25 μM DHO, and 60 μM resazurin. The assay involved two steps: (i) an enzymatic step over the course of 1 h at 25 °C to allow the DHODH-catalyzed oxidation of DHO to ORO and the conversion of resazurin to resorufin and (ii) the addition of 5 mM of stop mixture (100 mM HEPES and 10 mM ORO) and detection of the fluorescent signal emitted by resorufin. A DMSO-only (no inhibitor) control was used to establish 100% DHODH activity. Compound **3** was used as a positive control for DHODH inhibition at 1 μM. Percent DHODH activity was measured in duplicate for all ChemBridge compounds at three different concentrations depending on the ranking group from which the compound originated (see Supporting Information). DHODH activity for all 79 compounds in group 1 was evaluated at 1, 10, and 50 μM compound concentration. DHODH activity for the other 97 compounds in group 2 was evaluated at 10, 50, and 100 μM compound concentration. Biochemical IC_{50} was measured for compound **3** ($IC_{50,\ DHODH}$ = 1.06 nM) only during this initial characterization starting at 1 μM using a 3-fold serial dilution to a final concentration of 0.05 nM, yielding 10 data points.

https://doi.org/10.1021/acs.jcim.3c01358
J. Chem. Inf. Model. 2024, 64, 435−448

Biochemical IC_{50} Characterization. We characterized biochemical IC_{50} ($IC_{50,\ DHODH}$) for compounds that reduced the enzyme activity to less than 65% at the highest concentration evaluated during the initial enzyme activity assay. A fluorescence-based activity assay was repeated for 116 compounds that met this criterion. Compounds were tested in duplicate 10-dose IC_{50} mode using 3-fold serial dilutions starting at 10, 30, 50, or 100 μM against human DHODH by Reaction Biology Corporation (Malvern, PA, USA). Starting concentrations for IC_{50} measurements were based on the initial enzyme activity measurements for the selected compounds. For IC_{50} characterization, a fluorescence-based enzymatic activity assay was conducted under the same conditions as described above. Compound **3** was again used as a positive control for DHODH inhibition and was evaluated in a duplicate 10-dose IC_{50} mode using 3-fold serial dilutions starting at 1 μM ($IC_{50,\ DHODH}$ = 1.17 nM). Additionally, two negative controls were used in these experiments: (i) a no-inhibitor control to establish a baseline for 100% DHODH activity and (ii) compound **3** with no enzyme. It was possible to fit the sigmoidal dose response curves to the Hill equation for 20 of the 116 compounds, for which a 10-dose regime was measured.

MOLM-13 Cell Viability Assay. Cellular IC_{50} ($IC_{50,\ MOLM\text{-}13}$) was evaluated for the 20 compounds that showed a sigmoidal response during biochemical IC_{50} measurements. The purpose of the cellular characterization was to gain early insights into the serum shift effects for these compounds to aid in further lead optimization efforts. A cell viability MTS assay was conducted by Reaction Biology Corporation (Malvern, PA, USA). Staurosporine was purchased from Sigma-Aldrich (St. Louis, MI, USA) as a positive control reference. Cell viability was measured relative to that of a DMSO-only control. CellTiter 96 Aqueous One Solution Reagent was obtained from Promega (Madison, WI, USA) and was used as the MTS assay reagent. MOLM-13 cells were purchased from AddexBio (Pittsburgh, PA, USA) and were cultured in RPMI-1640 media supplemented with 10% fetal bovine serum (FBS), 10 μg/mL penicillin, and 100 μg/mL streptomycin. Cell cultures were maintained at 37 °C under a humidified atmosphere of 5% CO_2. The compounds were tested in a duplicate 10-dose IC_{50} mode starting at a concentration of 30 μM, except compound **16** for which we used a starting concentration of 10 μM due to the potent response observed for this compound during biochemical IC_{50} characterization. A starting concentration of 1 μM was used for the staurosporine control. 25 μL of culture medium containing 5000 MOLM-13 cells were delivered to each well of a 384-well plate. Approximately 20 min after cells were added, 5 μL of each compound was added to the wells. The plate was allowed to incubate at 37 °C for 96 h before 6 μL of the MTS reagent was added. Cells were incubated for an additional 2.5 h at 37 °C following the addition of the MTS reagent, and then absorbance at 492 nm was read using an Envision 2104 Multilabel Reader. The presence of viable cells in each well was determined qualitatively by observing a colored formazan product. IC_{50} was calculated by fitting data to the Hill equation. If a fit to the Hill equation was not possible, we attempted to extrapolate IC_{50} from a fit to a sigmoid function.

Computational ADMET Predictions. We used the QikProp program in Schrödinger to obtain a preliminary estimate of ADME data for our successfully identified DHODH inhibitors. The normal evaluation option was selected instead of the fast option. If more than one prediction was returned for a single compound, then the option with the least amount of ADME outliers was selected based on the "#stars" descriptor. If duplicate predictions had the same value for the "#stars" descriptor, then the prediction with the lowest SASA was used. We focused specifically on descriptors that pertain to solubility, lipophilicity, and cell permeability for this preliminary assessment. As a secondary assessment, with a stronger focus on toxicology, we also evaluated these properties using the admetSAR Web server for compounds **11**−**30**.

RESULTS

AML is a complex and prevalent disease with limited treatment options. AML becomes exponentially more difficult to treat in elderly populations, who frequently cannot tolerate aggressive cytotoxic chemotherapies, which are currently used as the standard-of-care. The discovery of DHODH as a target for differentiation therapy in AML cases has been encouraging, but few drugs have proven to be efficacious in treating this disease. Unexpected side effects perturb therapeutic applications for even the most promising DHODH inhibitors. The need to identify novel inhibitors remains critical, with the ultimate goal being the discovery of a lead that can be successfully administered in a clinical setting. In this work, we conducted a high-throughput virtual screening of the ChemBridge EXPRESS-pick library to rapidly identify new compounds with potential to act as DHODH inhibitors. We selected molecules with favorable drug-like features in the earliest stages of the drug discovery pipeline to promote future lead optimization efforts. Remarkably, our results were obtained without conducting enhanced sampling of the 6ET4 crystal structure. Two distinctly different groups of compounds were derived from virtual screening: one with the most promising compounds by docking score (EXPRESS Library "group 1"; 79 compounds total) and another with compounds selected based on predicted ligand efficiency (EXPRESS Library "group 2"; 97 compounds total). In general, entries selected by the docking score tended to be much larger and more nonpolar than those ranked by ligand efficiency. Guided by in silico predictions, we initially characterized 176 compounds with an enzyme activity assay, followed by IC_{50} measurement in vitro. This isolated 20 novel DHODH inhibitors with biochemical IC_{50} values that ranged from 91 nM to 54 μM. We were able to determine cellular IC_{50} values for 10 of these 20 inhibitors that ranged from 2.3 to 50.6 μM in MOLM-13 cells. A discussion is presented for the most promising compounds identified in this work: compounds **16** and **17**.

Self-Docking Assessments. We selected a DHODH conformation to use for molecular docking based on in-place rmsd comparisons from a self-docking procedure. We hypothesized that if Glide SP could accurately reproduce experimentally determined binding poses for a cocrystallized ligand, then this would likely increase its chances to reliably predict binding poses for novel DHODH inhibitors. We performed self-docking on PDB IDs 1UUO, 2WV8, 3ZWT, 4OQV, 5H2Z, 1D3H, 5MVC, 6ET4, 6OC0, 6QU7, 2BXV, 2FPT, 2FPV, 2FPY, and 3U2O and calculated in-place rmsds for each respective cocrystallized inhibitor to evaluate predictive accuracy for each model (Figure S1). 2BXV, 2FPT, 2FPV, 2FPY, and 3U2O were evaluated retroactively after docking was performed. All but three DHODH models (5H2Z, 6OC0, and 2BXV) met our in-place rmsd cutoff of 2.0

https://doi.org/10.1021/acs.jcim.3c01358
J. Chem. Inf. Model. 2024, 64, 435−448

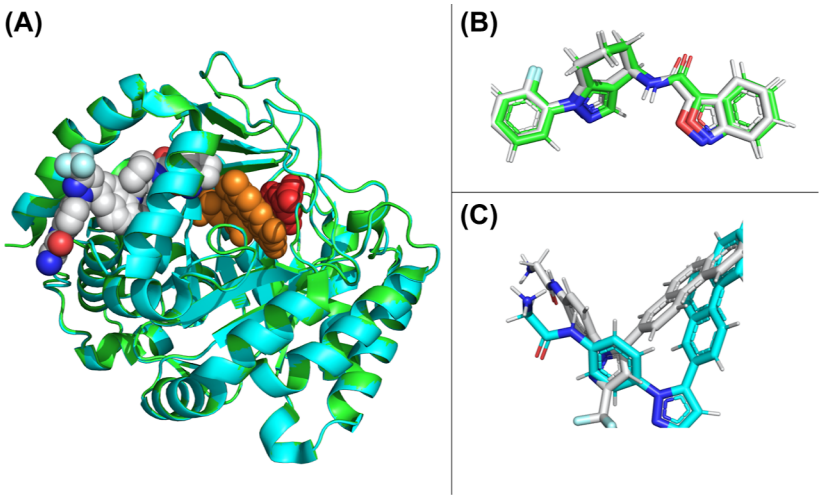

Figure 3. (A) Superimposition of the best (6ET4, green) and worst (6OC0, cyan) performing DHODH structures from self-docking assessments. FMN and DHO are represented by orange and red spheres, respectively. An inhibitor bound to the ubiquinone binding site is shown with gray spheres. The all-atom rmsd between these two structures is 0.7 Å. Other panels illustrate a superimposition of the cocrystallized inhibitors (gray) with the Glide SP predicted pose in (B) 6ET4 and (C) 6OC0.

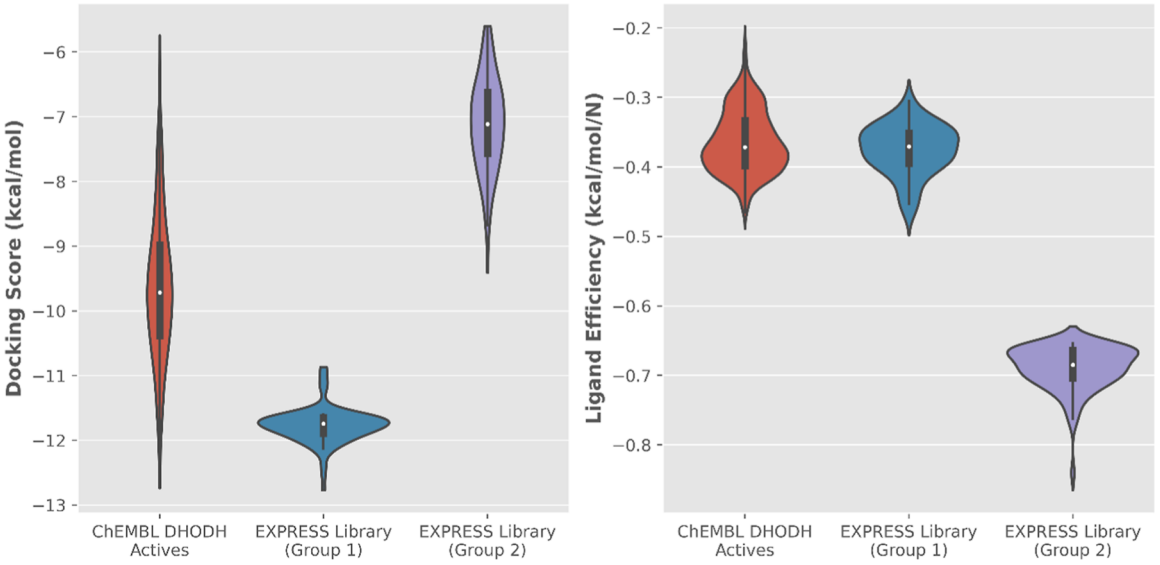

Figure 4. Summary of Glide SP virtual screening results. Data are shown for approximately 800 docked known DHODH inhibitors ("ChEMBL DHODH Actives"), the top 79 ChemBridge EXPRESS-pick compounds when ranked by docking score ("EXPRESS Library group 1"), and the top 97 ChemBridge EXPRESS-pick compounds when ranked by ligand efficiency ("Express Library group 2").

Å. Out of all of the models evaluated, the lowest and highest in-place rmsds were observed for 3U2O and 6OC0, respectively. However, 3U2O was one of the structures that was evaluated with self-docking after our initial round of in silico screening was complete. The second best in-place rmsd was for 6ET4, which is what we used for docking. While 3U2O does perform slightly better than 6ET4 by approximately 0.1 Å by in-place rmsd, 6ET4 was resolved at a higher resolution than 3U2O (1.7 vs 2.2 Å, respectively). Both are likely very suitable candidates to use for docking, but we used 6ET4 for all further data acquisition. Despite a large difference between the in-place rmsds calculated for the cocrystallized inhibitors in 6ET4 versus 6OC0, both structures were resolved in very similar conformations with a mutual rmsd of 0.7 (Figure 3A). Glide SP closely reproduced the crystal inhibitor conformation for 6ET4 (Figure 3B), but not that for 6OC0 (Figure 3C). Based on these results, we chose to use 6ET4 for all virtual screening experiments reported here.

Virtual Screening Results. We used Glide SP to dock a total of 461,106 LigPrepped small molecules from the ChemBridge EXPRESS-Pick library into 6ET4. We selected these compounds by prefiltering the EXPRESS library to remove any PAINS and Lipinski violators as well as any possible duplicate entries. A number of molecules evaluated in the EXPRESS library returned multiple predicted binding poses, but we considered only the lowest-scoring conformer. We hypothesized that the docking score and/or ligand efficiency would be reliable indicators of DHODH binding. We obtained two distinctly different lists of DHODH inhibitor candidates by extracting the molecules with either lowest docking score (EXPRESS Library "group 1") or lowest ligand efficiency (EXPRESS Library "group 2") (Figure 4). As a basis for comparison, we docked approximately 800 previously

https://doi.org/10.1021/acs.jcim.3c01358
J. Chem. Inf. Model. 2024, 64, 435−448

reported DHODH inhibitors of similar sizes, including compounds **1**−**10**, from the ChEMBL database. The docking scores for the known actives ranged from −3.78 to −12.74 kcal/mol, with a mean docking score of −9.53 ± 1.12 kcal/mol. Almost all of the compounds in group 1, but not group 2, had better docking scores when compared against scores for known inhibitors. The docking scores for the most potently predicted compounds in group 2 were comparable to the mean docking score for known inhibitors. However, the vast majority of group 2 performed poorly when judged by the docking score. Ligand efficiency was also evaluated to standardize docking scores against the size of each docked compound by penalizing molecules with a higher number of heavy atoms. The ligand efficiencies for the known actives and group 1 were highly comparable, but the entirety of group 2 had better ligand efficiencies than any of the known inhibitors or compounds from group 1. In general, the docking score tended to favor larger, nonpolar compounds (average MW = 434 g/mol; average log P = 4.83) that had a higher proclivity to form interactions with various residues in the DHODH binding pocket. We postulate that this observation was attributed to the presence of aromatic rings in these molecules that could form favorable $\pi-\pi$ stacking interactions within the binding pocket. On the contrary, ligand efficiency tended to favor smaller, hydrophilic compounds (average MW = 163 g/mol; average log P = 1.07) by selecting against compounds with more heavy atoms that may have attributed to a seemingly favorable docking score. We elected to advance groups 1 and 2 for experimental validation to attain a better understanding of which metric is a more reliable indicator of novel inhibitor candidates.

We refined our selection of novel inhibitor candidates after our initial evaluations of groups 1 and 2 with Glide SP were complete. Exceptionally small molecules with a MW less than 130 g/mol were eliminated, and this condition exclusively affected compounds in group 2. Five compounds in group 1 (ChemBridge IDs 5431088, 5423221, 5428235, 5429054, and 5425727) contained phenylpiperazinyl methyl (PPM) with a terminal pyrene. Although we considered the PPM component of these structures an attractive structural feature, we were concerned about the large, bulky pyrene group because this may increase the likelihood for nonspecific binding. To address this, we substituted pyrene in these structures with naphthalene and biphenyl groups and obtained docking scores for these modifications. Not all naphthyl and biphenyl analogs evaluated were part of the EXPRESS library, but all were readily available through ChemBridge. Docking scores were less favorable for all biphenyl and naphthyl substitutions compared with the original pyrene structures. However, an improvement in ligand efficiency was observed for the 2-naphthyl substitutions (Table S1), which is what we ultimately replaced these five compounds with. We visually inspected the docked poses of all 176 compounds selected based on either the docking score or ligand efficiency to confirm docking into the active site of DHODH. All 176 compounds were subsequently ordered from ChemBridge for in vitro characterization (Table S2). We retrospectively repeated docking of the EXPRESS library by removing ORO from the 6ET4 structure to evaluate how ORO influenced our original docking assessment. Docking score and ligand efficiency increased and became less favorable for essentially every molecule when ORO was excluded (Figure S7). ORO likely benefited docking by providing additional interactions for the docked ligand in the ubiquinone tunnel.

Experimental Validation. We experimentally validated the inhibition potential for the 176 compounds that performed best in silico by first measuring the DHODH activity in a fluorescence-based assay across three concentrations. A baseline for 100% DHODH activity was established using a negative control where reaction buffer was titrated in place of an inhibitor. Additionally, a "no enzyme" negative control was also conducted in parallel with the "no inhibitor" negative control. 116 of these 176 compounds reduced DHODH activity to less than 65% at the highest concentration evaluated in the initial activity assessment and advanced to further characterization in vitro. A sigmoidal response was observed for 20 of the 116 compounds that met the 65% activity cutoff, which allowed for the determination of biochemical IC_{50}. Compound **3** was used as a positive control during the biochemical IC_{50} determinations. Another "no enzyme" trial was used during biochemical IC_{50} measurements as a negative control. Five of the 20 compounds originated from group 2 (Figure 5) and 15 compounds originated from group 1 (Figure 6). Finally, we assessed possible serum protein shift effects for these 20 compounds by measuring the cellular IC_{50} in a viability assay with MOLM-13 cells. Compound **3** was again used as a positive control in the cellular assays. Additionally, staurosporine was used as a separate positive control in the cellular experiments. A cellular IC_{50} could be detected for only 10 of these 20 compounds. Compounds **16** and **17** exhibited the strongest biochemical and cellular IC_{50} measurements, respectively.

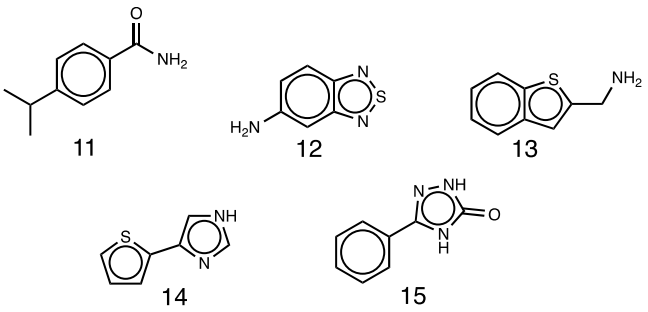

Figure 5. 2D structures of ChemBridge compounds selected by ligand efficiency that exhibited some degree of DHODH inhibition in vitro.

60 of the compounds evaluated during the initial activity assay failed to reduce DHODH activity to below 65% at the highest concentration tested. 51 of these compounds originated from group 2 and 9 compounds were from group 1. We conducted experiments to determine the biochemical IC_{50} on 70 compounds from group 1 and 46 compounds from group 2 that did perturb DHODH activity during our initial assessment. However, biochemical IC_{50} could only be determined for five compounds from group 2, with values that ranged between 10.9 and 53.8 μM (Table 1). A cellular IC_{50} value >10,000 μM was measured for all compounds in group 2. We hypothesize that the lack of inhibition observed for the group 2 compounds can be attributed to the small size of these molecules. All five group 2 compounds that we did measure a biochemical IC_{50} for contained conjugated aromatic rings, which could increase the likelihood of forming favorable interactions within the binding site of DHODH. However, all five compounds also contained hydrogen bond acceptors that

https://doi.org/10.1021/acs.jcim.3c01358
J. Chem. Inf. Model. 2024, 64, 435−448

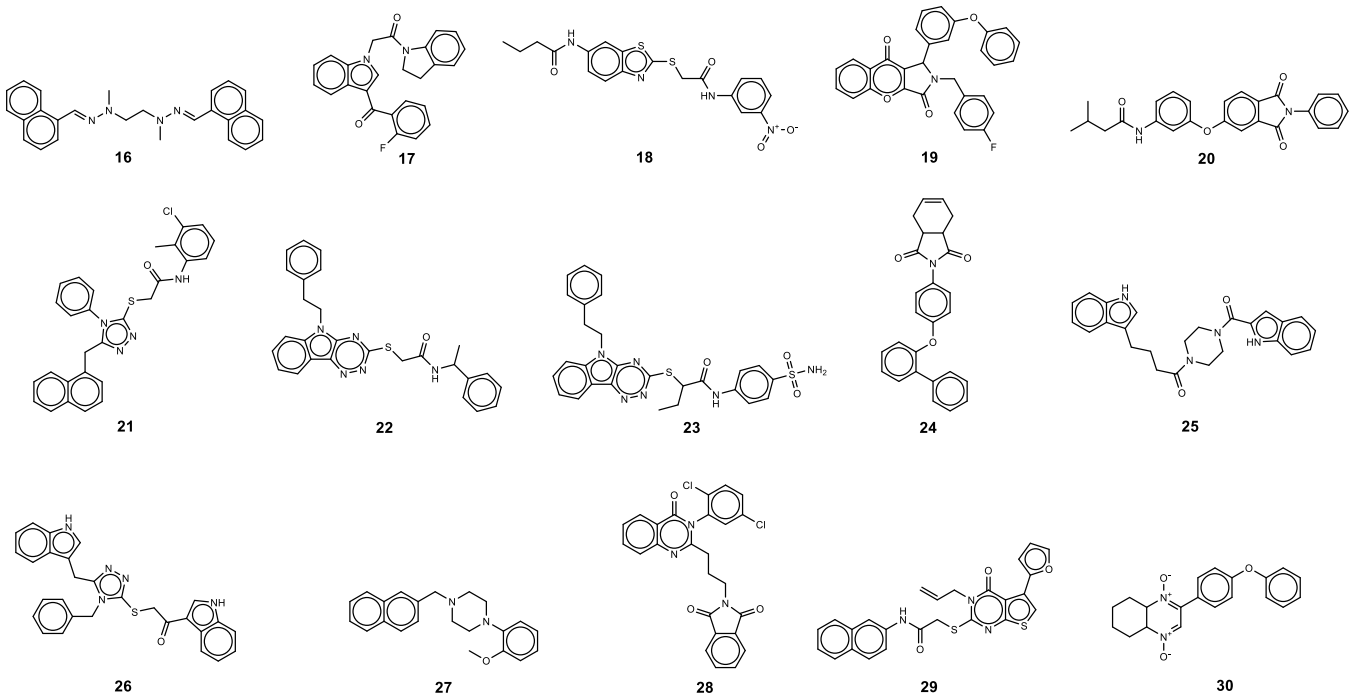

Figure 6. 2D structures of ChemBridge compounds selected by the docking score that inhibited DHODH activity in vitro.

Table 1. Computational and Experimental Measurements for Compounds 11−15 from Group 2, which was Ranked Based on Ligand Efficiency

compound no.	ChemBridge ID	docking score (kcal/mol)	ligand efficiency (kcal/mol)	$IC_{50,\ DHODH}$ (μM)	$IC_{50,\ MOLM\text{-}13}$ (μM)
11	9139246	−7.854	−0.654	10.9 ± 1.2	>10,000
12	4031207	−6.587	−0.659	13.6 ± 2.0	
13	4100819	−7.226	−0.657	17.2 ± 1.8	
14	4034945	−6.799	−0.680	17.9 ± 2.5	
15	9292094	−8.108	−0.676	53.8 ± 8.4	

Table 2. Computational and Experimental Measurements for Compounds 16−30 from Group 1, which was Ranked Based on Docking Score[a]

compound no.	ChemBridge ID	docking score (kcal/mol)	ligand efficiency (kcal/mol/N)	$IC_{50,\ DHODH}$ (nM)	$IC_{50,\ MOLM\text{-}13}$ (μM)
16	5538705	−11.644	−0.388	91.0 ± 9.5	>10,000
17	7907504	−11.652	−0.388	391.9 ± 55.4	2.3 ± 0.004
18	7689962	−11.672	−0.402	448.8 ± 155.2	>10,000
19	7870764	−12.768	−0.355	596.6 ± 88.5	17.5 ± 8.3
20	6094366	−11.960	−0.386	607.7 ± 62.6	>10,000
21	7628744	−11.676	−0.334	665.7 ± 78.8	11.5 ± 1.3
22	6327207	−11.963	−0.352	888.3 ± 147.1	29.2 ± 0.2
23	6314397	−11.599	−0.305	1001 ± 134.2	21.8 ± 17.3
24	7417142	−11.663	−0.389	1014 ± 7.8	50.6 ± 21.4
25	9322249	−11.840	−0.382	1513 ± 80.6	5.2 ± 0.2
26	7511661	−11.733	−0.335	1698 ± 164.0	14.4 ± 0.5
27	5261206	−10.888	−0.436	1946 ± 342.9	13.8 ± 3.5
28	7132801	−11.662	−0.353	2197 ± 232.6	>10,000
29	7595599	−11.805	−0.358	2612 ± 1242	>10,000
30	7925560	−11.705	−0.468	2742 ± 252.4	12.6 ± 2.3

[a]A curve fit could not be established for blank cells.

could make these more likely to interact nonspecifically. Despite this presence of hydrogen bond acceptors, none of these compounds violated more than one of Lipinski's Rule of Five or contained PAINS functional groups. It is possible that raising the MW cutoff to a value greater than 130 g/mol or allowing zero Lipinski violations may improve the success of identifying potential DHODH inhibitors by ligand efficiency alone. Since ligand efficiency penalizes larger compounds with a higher number of heavy atoms, we were not surprised that group 2 did contain several low-MW compounds. We used ligand efficiency in this work as a secondary metric to the docking score in identifying potent ligand precursors. As such,

https://doi.org/10.1021/acs.jcim.3c01358
J. Chem. Inf. Model. 2024, 64, 435−448

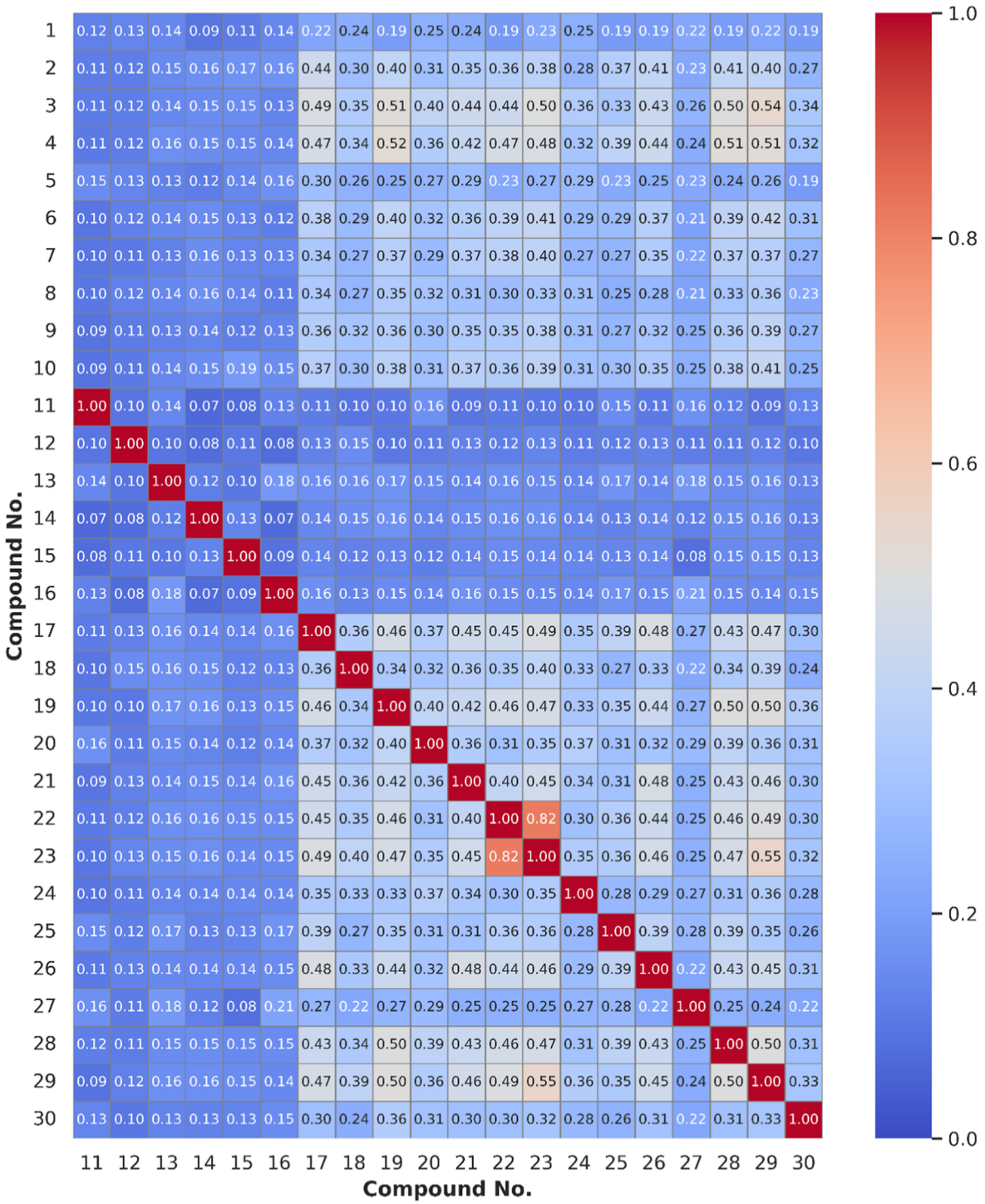

Figure 7. Pairwise Tanimoto indices between the cocrystallized DHODH inhibitors used for self-docking (compounds **1**−**10**), which do not encompass an exhaustive list of DHODH inhibitors, and the compounds that an IC_{50} value was determined for during experimental validation (compounds **11**−**30**).

ligand efficiency serves as a better indicator of which compounds could be further optimized and is best for making comparisons between similarly sized structures.

Small molecules originating from group 1 were much more successful at inhibiting DHODH than those in group 2. Biochemical IC_{50} values were measured between 91 nM and 2.7 μM for 15 of the compounds originating from group 1 (Table 2). All 15 of these compounds reduced DHODH activity to 65% or lower at a concentration of 1 μM during the initial activity assessment, which far exceeded our described cutoff criterion based on the activity at the highest evaluated concentration of 50 μM for these compounds. Cellular IC_{50} values were measured between 2.3 and 50.6 μM for 10 of these 15 compounds (Table 2). Compound **17** had the best cellular IC_{50} of 2.3 μM and the second best biochemical IC_{50} of 392 nM, which we claim makes this molecule the most promising DHODH inhibitor presented in this work. Compound **16** had the most potent biochemical IC_{50} of 91 nM but had

https://doi.org/10.1021/acs.jcim.3c01358
J. Chem. Inf. Model. 2024, 64, 435−448

inconclusive results during the cell viability assay. The lack of cellular activity for compound **16** could be attributed to the symmetrical structure of this compound as well as the presence of Schiff bases. Notably, Schiff bases in particular are chemically reactive, which could have led to the formation of an unexpected byproduct that could not allow for DHODH inhibition. Alternatively, Schiff bases can also modify protein structures by reacting with amino acids. These effects may have culminated in unexpected promiscuous activity of compound **16** during the cellular characterization. Both compounds **17** and **16** reduced DHODH activity to approximately 15.6 and 8.8%, respectively, at 1 μM, and originated from group 1. These findings suggest that the docking score is a stronger indicator of possible DHODH inhibitors over ligand efficiency alone.

During our self-docking assessments, we used compounds **5** and **6**. Experimental validation revealed that compound **16** had a better biochemical IC_{50} than compound **5** ($IC_{50,\ DHODH}$ = 0.21 μM[19]) and compound **6** ($IC_{50,\ DHODH}$ = 1.6 μM[62]) by 2.3- and 17.6-fold, respectively. Compound **5** has been reported as a brequinar-like inhibitor that occupies the same position in the ubiquinone binding site, but, unlike compound **2**, is not sterically hindered by a methyl group at the *ortho* position of its aromatic ring.[19] Indeed, compound **5** is structurally unique from compound **2**. We calculated a Tanimoto index of 0.31 between compounds **2** and **5**. Fritzson and colleagues proposed that this extra rotational freedom facilitates more optimal interactions between compound **5** and conserved DHODH residue R136. Based on the docked pose, it is possible that compound **16** is an improvement over compound **5** in terms of biochemical IC_{50} and structural similarity to compound **2** (Figure 7). It is worth noting here that compounds **1**−**10** are not an exhaustive list of DHODH inhibitors, but included in this subset are several highly potent and selective compounds for DHODH inhibition. It is reasonable to hypothesize that the central alkane bond in compound **16** would allow for significant conformational flexibility that may have contributed to these improvements over compound **5**. Compound **6** has also been reported to occupy the same binding site as compound **2** in multiple DHODH isoforms facilitated by H-bond interactions with R136.[62] However, compound **6** did not potently inhibit DHODH. The biochemical IC_{50} for compound **17** was better by 4.1-fold compared to compound **6**. It is possible that similar interactions with conserved residues, such as R136, occurred for compound **17** due to the rotational flexibility of prosthetic groups that stem from the central indole ring of this inhibitor. Furthermore, the predicted protein−ligand interactions that contribute to GlideScore are not pairwise-decomposable. This makes it impossible to validate the contributions from specific atoms in the docked ligand or in the receptor. It is possible, however, to calculate per-residue interaction scores between a molecule and residues in the receptor grid. To better understand the types of interactions we might expect with compounds **16** and **17**, we assessed the H-bond interaction scores as a function of minimum distance to R136 (in the docked pose) for compounds **1**−**30** (Figure S2). It was not surprising that ligands predicted to bind closer to R136, such as compounds **2** and **5**, have the lowest and most favorable H-bond interaction scores. Compounds **16** and **17** were predicted to bind around 1.9 and 2.2 Å away from R136, respectively, but a nonzero H-bond interaction score was only observed for compound **16**. We suspect that an H-bond interaction score of zero was calculated for compound **17** because all H-bond acceptors in the ligand are facing away from R136 in the docked pose. The H-bond interaction score between compound **16** and R136 was 1.9-fold worse than that of compounds **2** and **5**. Interestingly, compound **6** bound at a comparable distance of 2.0 from R136, but had an improved H-bond interaction score compared to compound **16** (by 1.1-fold). Thus, we do not expect R136 to provide significant intermolecular interactions that mediate an improved biochemical IC_{50} for compounds **16** and **17**, as has been reported for previously identified inhibitors. The principal interactions behind this observation most likely come from other residues in the ubiquinone binding site.

Even though ligand efficiency did not predict inhibitor candidates well, it was useful in guiding our selection of naphthalene and biphenyl substitutions in the five PPM structures from group 1 that contained a terminal pyrene (Table S1). Prior to experimental validation, we chose not to screen against compounds with a large, bulky pyrene group because these are more likely to bind nonspecifically or have a significant serum protein shift effect in cellular assays. The PPM structures containing pyrene always had a more favorable docking score relative to the naphthyl and biphenyl substitutions because pyrene could participate in more intermolecular interactions within the ubiquinone pocket of DHODH. Ligand efficiency allowed us to standardize docking score to the size of each PPM substitution, clearly and quantitatively illustrating the 2-naphthyl analogue as the better option. Compound **27** is the only one of the five PPM compounds that demonstrated DHODH inhibition with a biochemical and cellular IC_{50} of 1.9 and 13.8 μM, respectively. The other four PPM structures (compounds **45**, **61**, **62**, and **81**) did not demonstrate DHODH inhibition in vitro (Table S2). Although compound **27** lacked potency, this could be compensated through future lead optimization efforts by studying structure−activity relationships (SAR).

Ligand-Based Evaluations. Following experimental confirmation of our DHODH inhibitors, we returned to the Schrödinger suite to computationally predict the ADMET properties for compounds **11**−**30** using QikProp and admetSAR (Table S3 and Supporting Information 2). The latter was included to supplement QikProp predictions, which do not heavily focus on toxicology. The primary observation made from admetSAR was that compounds **16** and **17** may cause mitochondrial toxicity but are not expected to be nephrotoxic or experience acute oral toxicity. Further development efforts using these structures will inevitably require investigation of such pharmaceutically relevant properties that were not an integral contribution toward the primary objective of this study (i.e., identifying inhibitors). QikProp and admetSAR are fast and computationally inexpensive ways to set an in silico benchmark for solubility, absorption, and toxicology. We calculated QPlogS predictions for compounds **11**−**30** (Figure S3) after employing a LigPrep procedure to generate conformers at pH 7.4 ± 1.0. Predictions for these measures should ideally have a value between −6.5 and 0.5 mol dm^{-3}. This was observed for compounds **16** and **17**, among others. Group 1 compounds generally had a higher predicted aqueous solubility than group 2 compounds. We also calculated the octanol−water partition coefficient (log *P*) (Figure S4). QikProp recommends a log *P* (QP log *P*) range between −2.0 and 6.5, with higher values denoting more hydrophobicity. These values are in consonance with good

https://doi.org/10.1021/acs.jcim.3c01358
J. Chem. Inf. Model. 2024, 64, 435−448

solubility profiles for our compounds, which was substantiated experimentally.

To complement our experimental assessment with MOLM-13 cells, we also evaluated the permeability using QikProp. The program models transport across the gut-blood and blood−brain barriers based on predicted Caco-2 and MDCK cell permeability. For both models, QikProp suggests that predicted rates in excess of 500 nm/s denote good permeability. In the Caco-2 model, only compounds **15**, **18**, **23**, and **25** had predicted permeability rates of less than 500 nm/s (Figure S5). All permeability rates predicted by the MDCK model were lower than those predicted by the Caco-2 model, which is consistent with what we would have expected for these barriers (Figure S6). Compound **16** had the highest predicted permeability rates of 7924 and 4634 nm/s in both the Caco-2 and MDCK models, respectively. Several compounds had predicted permeability rates greater than 1000 nm/s. These favorable predictions for compounds **16** and **17** further support continued development efforts toward these structures as DHODH inhibitors. Unfortunately, these results did not explain why a cellular IC_{50} could not be measured for compound **16** in the MOLM-13 assay. If anything, they suggest that a lack of cell permeability is likely not the cause of our inability to measure the cellular IC_{50} values for some compounds. A clear explanation for this phenomenon remains elusive. It is possible that the symmetric azide bonds in compound **16** experience cleavage under acidic conditions. Another more likely possibility is that compound **16** binds DHODH nonspecifically and interacts with proteins present in FBS or within the cell itself. Compound **17** was not subject to similar effects, even though it had a worse IC_{50} than compound **16** during biochemical characterizations.

Finally, we assessed the relative 2D structural similarity for all compounds that an IC_{50} was measured for by calculating pairwise Tantimoto indices (Figure 7). This assessment suggested that the hits reported in this work are structurally unique from the known DHODH inhibitors used in self-docking (compounds **1**−**10**) and from one another. A notable exception, however, was between compounds **22** and **23**, which had a pairwise Tanimoto index of 0.82. All other compounds had a Tanimoto index of 0.55 or less, which fell below our cutoff value for similarity. Out of all our hits, compound **29** and compound **3** (BAY 2402234) had the highest similarity with a Tanimoto index of 0.54. Compounds **11**−**15** from group 2 had the lowest pairwise Tanimoto indices. Additionally, the most successful hits (compounds **11**−**30**) tended to carry symmetric and heterocyclic features in their structure.

To summarize, we present 20 novel DHODH inhibitors that have been validated in vitro by determination of IC_{50}; 15 inhibitors from group 1 and five from group 2. 10 of the 15 inhibitors from group 1 perturbed the survival of MOLM-13 cells. None of the inhibitors from group 2 reduced MOLM-13 cell viability; however, the high ligand efficiency of these compounds does indicate space for further optimization. It is probable that some degree of improvement could be observed by carefully increasing the molecular weight of group 2 compounds in future directions. Such changes should be introduced rationally to allow for target-specific optimization with DHODH. Additionally, group 2 in its current form could serve as a starting point for fragment-based drug design (FBDD) efforts. A high ligand efficiency does most often depend on ligand size, so the output of a potential FBDD approach would likely lower ligand efficiency at the cost of improved efficacy as a DHODH inhibitor.[63,64] Compounds **16** and **17** were the most potent inhibitors out of all of the other compounds evaluated in this work. The biochemical IC_{50} for compound **16** ($IC_{50,\ DHODH}$ = 91 nM) was better by more than 4-fold compared to that of compound **17** ($IC_{50,\ DHODH}$ = 392 nM). However, the cell viability assay was inconclusive for compound **16**. Compound **17** ($IC_{50,\ MOLM\text{-}13}$ = 2.3 μM) was >2-fold more potent than the next best hit from the cellular viability assay, compound **25**.

CONCLUSIONS

The mitochondrial enzyme, DHODH, is a pivotal component in *de novo* pyrimidine biosynthesis.[15] Cancerous myeloid progenitors, such as those implicated in AML, vitally rely on this pathway to provide the necessary energy for abnormally increased proliferation rates.[12,14] The therapeutic potential of inhibiting *de novo* pyrimidine biosynthesis by targeting DHODH has been a research focus for decades.[16] Unfortunately, many known compounds that inhibit DHODH have adverse side effects that significantly attenuate their therapeutic potential or warrant further investigation.[3,4] There remains strong interest in identifying novel inhibitors that can act alone or synergistically with other treatments to improve AML survival rates. We used SBDD to augment the process of drug discovery and lead optimization.

Through our virtual screening approach, we successfully identified 20 structurally diverse DHODH inhibitors, 10 of which had μM potency in MOLM-13 cells. The most potent inhibitors reported here include compounds **16** and **17**, which are both symmetric and aromatic compounds. These structural features could be used as novel scaffolds for future molecules that may even more potently inhibit DHODH. Compound **16** had the best biochemical IC_{50} of 91 nM and also exceeded the biochemical IC_{50} of three well-known DHODH inhibitors that were used in our initial self-docking assessments: compound **1** ($IC_{50,\ DHODH}$ = 130 nM), compound **5** ($IC_{50,\ DHODH}$ = 210 nM), and compound **6** ($IC_{50,\ DHODH}$ = 1.6 μM). Although the biochemical IC_{50} for compound **17** was more than 4-fold lower than that of compound **16**, compound **17** performed the best in our cell viability assay relative to the other hits ($IC_{50,\ MOLM\text{-}13}$ = 2.3 μM). Future work will focus on resolving the DHODH structure in complex with compounds **16** and **17** to gain a better understanding of the principal interactions that drive binding of these inhibitors. Nonetheless, compounds **16** and **17** have great potential to act as scaffolds for future inhibitors. We also feel that it is important to address the rather small size of the EXPRESS pick library. While we did successfully identify novel DHODH inhibitors in this work, an alternative strategy would have been to consider ultra large compound libraries with millions, or preferably billions, of compounds by implementing machine learning/deep learning techniques.[65−67] This could have increased the likelihood that more inhibitors would have been identified from our initial round of screening. Even so, this could have increased our chances of identifying potential false positives. The EXPRESS library has been curated to represent drug-like molecules, which does allow us to still draw meaningful conclusions in the presented form.

In summary, we found that the docking score was a strong indicator of small molecules that had potential to act as DHODH inhibitors in vitro. Ligand efficiency appeared to have a bias for smaller amphipathic molecules that likely

https://doi.org/10.1021/acs.jcim.3c01358
J. Chem. Inf. Model. 2024, 64, 435−448

interact nonspecifically. Docking score better selected for molecules with poses that more completely occupied the entire DHODH binding pocket. Future work will focus on SAR of these hits and will evaluate the accuracy of our docked poses using experimentally determined structures cocrystallized with these inhibitors. Already, the hits reported in this work provide encouraging drug candidates for the inhibition of DHODH and may eventually lead to discoveries with implications for the treatment of AML.

■ ASSOCIATED CONTENT

Supporting Information

The Supporting Information is available free of charge at https://pubs.acs.org/doi/10.1021/acs.jcim.3c01358.

Modeling information, structural modifications, qH[1]NMR or LCMS spectra, all SMILES strings, and raw data from the biochemical and cellular curve fits for compounds **16** and **17** (PDF)
(ZIP)

■ AUTHOR INFORMATION

Corresponding Author

Steffen Lindert − *Department of Chemistry and Biochemistry, Ohio State University, Columbus, Ohio 43210, United States;* orcid.org/0000-0002-3976-3473; Phone: 43210 614-292-8284; Email: lindert.1@osu.edu; Fax: 614-292-1685

Authors

William T. Higgins − *Department of Chemistry and Biochemistry, Ohio State University, Columbus, Ohio 43210, United States*

Sandip Vibhute − *Medicinal Chemistry Shared Resource, Comprehensive Cancer Center, Ohio State University, Columbus, Ohio 43210, United States*

Chad Bennett − *Medicinal Chemistry Shared Resource, Comprehensive Cancer Center and Drug Development Institute, Ohio State University, Columbus, Ohio 43210, United States*

Complete contact information is available at: https://pubs.acs.org/10.1021/acs.jcim.3c01358

Author Contributions

W.H. and S.L. designed and conducted all virtual screening contributions, S.V. and C.B. designed experimental validation steps, W.H. wrote the original draft and created all figures, and all authors reviewed and/or proposed edits to the manuscript.

Notes

The authors declare no competing financial interest.

■ ACKNOWLEDGMENTS

The authors wish to acknowledge members of the Lindert lab for helpful discussions, the Ohio Supercomputer Center[68] for providing valuable computational resources, and the staff at Reaction Biology Corporation for their assistance in conducting experimental validation.

■ ABBREVIATIONS

DHODH, dihydroorotate dehydrogenase; AML, acute myeloid leukemia; DHO, L-dihydroorotate; FBS, fetal bovine serum; ORO, orotate; UMP, uridine monophosphate; FMN, flavin mononucleotide; SBDD, structure-based drug discovery; PPM, phenyl-piperazinyl methyl

■ REFERENCES

(1) Ferrara, F.; Schiffer, C. A. Acute myeloid leukaemia in adults. *Lancet* **2013**, *381* (9865), 484−495.

(2) Zhou, J.; Yiying Quah, J.; Ng, Y.; Chooi, J. Y.; Hui-Min Toh, S.; Lin, B.; Zea Tan, T.; Hosoi, H.; Osato, M.; Seet, Q.; Lisa Ooi, A. G.; Lindmark, B.; McHale, M.; Chng, W. J. ASLAN003, a potent dihydroorotate dehydrogenase inhibitor for differentiation of acute myeloid leukemia. *Haematologica* **2020**, *105* (9), 2286−2297.

(3) Christian, S.; Merz, C.; Evans, L.; Gradl, S.; Seidel, H.; Friberg, A.; Eheim, A.; Lejeune, P.; Brzezinka, K.; Zimmermann, K.; Ferrara, S.; Meyer, H.; Lesche, R.; Stoeckigt, D.; Bauser, M.; Haegebarth, A.; Sykes, D. B.; Scadden, D. T.; Losman, J. A.; Janzer, A. The novel dihydroorotate dehydrogenase (DHODH) inhibitor BAY 2402234 triggers differentiation and is effective in the treatment of myeloid malignancies. *Leukemia* **2019**, *33* (10), 2403−2415.

(4) Wu, D.; Wang, W.; Chen, W.; Lian, F.; Lang, L.; Huang, Y.; Xu, Y.; Zhang, N.; Chen, Y.; Liu, M.; Nussinov, R.; Cheng, F.; Lu, W.; Huang, J. Pharmacological inhibition of dihydroorotate dehydrogenase induces apoptosis and differentiation in acute myeloid leukemia cells. *Haematologica* **2018**, *103* (9), 1472−1483.

(5) Newell, L. F.; Cook, R. J. Advances in acute myeloid leukemia. *Bmj* **2021**, *375*, n2026.

(6) Sykes, D. B.; Kfoury, Y. S.; Mercier, F. E.; Wawer, M. J.; Law, J. M.; Haynes, M. K.; Lewis, T. A.; Schajnovitz, A.; Jain, E.; Lee, D.; Meyer, H.; Pierce, K. A.; Tolliday, N. J.; Waller, A.; Ferrara, S. J.; Eheim, A. L.; Stoeckigt, D.; Maxcy, K. L.; Cobert, J. M.; Bachand, J.; Szekely, B. A.; et al. Inhibition of Dihydroorotate Dehydrogenase Overcomes Differentiation Blockade in Acute Myeloid Leukemia. *Cell* **2016**, *167* (1), 171.

(7) Lewis, T. A.; Sykes, D. B.; Law, J. M.; Muñoz, B.; Rustiguel, J. K.; Nonato, M. C.; Scadden, D. T.; Schreiber, S. L. Development of ML390: A Human DHODH Inhibitor That Induces Differentiation in Acute Myeloid Leukemia. *ACS Med. Chem. Lett.* **2016**, *7* (12), 1112−1117.

(8) Munier-Lehmann, H.; Vidalain, P. O.; Tangy, F.; Janin, Y. L. On dihydroorotate dehydrogenases and their inhibitors and uses. *J. Med. Chem.* **2013**, *56* (8), 3148−3167.

(9) Hansen, M.; Le Nours, J.; Johansson, E.; Antal, T.; Ullrich, A.; Löffler, M.; Larsen, S. Inhibitor binding in a class 2 dihydroorotate dehydrogenase causes variations in the membrane-associated N-terminal domain. *Protein Sci.* **2004**, *13* (4), 1031−1042.

(10) Ladds, M.; van Leeuwen, I. M. M.; Drummond, C. J.; Chu, S.; Healy, A. R.; Popova, G.; Pastor Fernández, A.; Mollick, T.; Darekar, S.; Sedimbi, S. K.; Nekulova, M.; Sachweh, M. C. C.; Campbell, J.; Higgins, M.; Tuck, C.; Popa, M.; Safont, M. M.; Gelebart, P.; Fandalyuk, Z.; Thompson, A. M.; Svensson, R.; Gustavsson, A. L.; Johansson, L.; Färnegårdh, K.; Yngve, U.; Saleh, A.; Haraldsson, M.; D'Hollander, A. C. A.; Franco, M.; Zhao, Y.; Håkansson, M.; Walse, B.; Larsson, K.; Peat, E. M.; Pelechano, V.; Lunec, J.; Vojtesek, B.; Carmena, M.; Earnshaw, W. C.; McCarthy, A. R.; Westwood, N. J.; Arsenian-Henriksson, M.; Lane, D. P.; Bhatia, R.; McCormack, E.; Laín, S. A DHODH inhibitor increases p53 synthesis and enhances tumor cell killing by p53 degradation blockage. *Nat. Commun.* **2018**, *9* (1), 1107.

(11) Sporrij, A.; Zon, L. I. Nucleotide stress responses in neural crest cell fate and melanoma. *Cell Cycle* **2021**, *20* (15), 1455−1467.

(12) Cisar, J. S.; Pietsch, C.; DeRatt, L. G.; Jacoby, E.; Kazmi, F.; Keohane, C.; Legenski, K.; Matico, R.; Shaffer, P.; Simonnet, Y.; Tanner, A.; Wang, C. Y.; Wang, W.; Attar, R.; Edwards, J. P.; Kuduk, S. D. N-Heterocyclic 3-Pyridyl Carboxamide Inhibitors of DHODH for the Treatment of Acute Myelogenous Leukemia. *J. Med. Chem.* **2022**, *65* (16), 11241−11256.

(13) Pal, S.; Sharma, A.; Mathew, S. P.; Jaganathan, B. G. Targeting cancer-specific metabolic pathways for developing novel cancer therapeutics. *Front. Immunol.* **2022**, *13*, 955476.

(14) Sainas, S.; Giorgis, M.; Circosta, P.; Gaidano, V.; Bonanni, D.; Pippione, A. C.; Bagnati, R.; Passoni, A.; Qiu, Y.; Cojocaru, C. F.; Canepa, B.; Bona, A.; Rolando, B.; Mishina, M.; Ramondetti, C.; Buccinnà, B.; Piccinini, M.; Houshmand, M.; Cignetti, A.; Giraudo, E.; Al-Karadaghi, S.; Boschi, D.; Saglio, G.; Lolli, M. L. Targeting Acute Myelogenous Leukemia Using Potent Human Dihydroorotate Dehydrogenase Inhibitors Based on the 2-Hydroxypyrazolo[1,5-a]pyridine Scaffold: SAR of the Biphenyl Moiety. *J. Med. Chem.* **2021**, *64* (9), 5404−5428.
(15) Diao, Y.; Lu, W.; Jin, H.; Zhu, J.; Han, L.; Xu, M.; Gao, R.; Shen, X.; Zhao, Z.; Liu, X.; Xu, Y.; Huang, J.; Li, H. Discovery of diverse human dihydroorotate dehydrogenase inhibitors as immunosuppressive agents by structure-based virtual screening. *J. Med. Chem.* **2012**, *55* (19), 8341−8349.
(16) Liu, S.; Neidhardt, E. A.; Grossman, T. H.; Ocain, T.; Clardy, J. Structures of human dihydroorotate dehydrogenase in complex with antiproliferative agents. *Structure* **2000**, *8* (1), 25−33.
(17) Baumgartner, R.; Walloschek, M.; Kralik, M.; Gotschlich, A.; Tasler, S.; Mies, J.; Leban, J. Dual binding mode of a novel series of DHODH inhibitors. *J. Med. Chem.* **2006**, *49* (4), 1239−1247.
(18) Davies, M.; Heikkilä, T.; McConkey, G. A.; Fishwick, C. W.; Parsons, M. R.; Johnson, A. P. Structure-based design, synthesis, and characterization of inhibitors of human and Plasmodium falciparum dihydroorotate dehydrogenases. *J. Med. Chem.* **2009**, *52* (9), 2683−2693.
(19) Fritzson, I.; Svensson, B.; Al-Karadaghi, S.; Walse, B.; Wellmar, U.; Nilsson, U. J.; da Graça Thrige, D.; Jönsson, S. Inhibition of human DHODH by 4-hydroxycoumarins, fenamic acids, and N-(alkylcarbonyl)anthranilic acids identified by structure-guided fragment selection. *ChemMedChem* **2010**, *5* (4), 608−617.
(20) Pally, C.; Smith, D.; Jaffee, B.; Magolda, R.; Zehender, H.; Dorobek, B.; Donatsch, P.; Papageorgiou, C.; Schuurman, H. J. Side effects of brequinar and brequinar analogues, in combination with cyclosporine, in the rat. *Toxicology* **1998**, *127* (1−3), 207−222.
(21) Burris, H. A., 3rd; Raymond, E.; Awada, A.; Kuhn, J. G.; O'Rourke, T. J.; Brentzel, J.; Lynch, W.; King, S. Y.; Brown, T. D.; Von Hoff, D. D. Pharmacokinetic and phase I studies of brequinar (DUP 785; NSC 368390) in combination with cisplatin in patients with advanced malignancies. *Invest. New Drugs* **1998**, *16* (1), 19−27.
(22) Jones, S. W.; Penman, S. L.; French, N. S.; Park, B. K.; Chadwick, A. E. Investigating dihydroorotate dehydrogenase inhibitor mediated mitochondrial dysfunction in hepatic in vitro models. *Toxicol. In Vitro* **2021**, *72*, 105096.
(23) Pattnaik, P. Surface plasmon resonance: applications in understanding receptor-ligand interaction. *Appl. Biochem. Biotechnol.* **2005**, *126* (2), 079−092.
(24) Madak, J. T.; Cuthbertson, C. R.; Miyata, Y.; Tamura, S.; Petrunak, E. M.; Stuckey, J. A.; Han, Y.; He, M.; Sun, D.; Showalter, H. D.; Neamati, N. Design, Synthesis, and Biological Evaluation of 4-Quinoline Carboxylic Acids as Inhibitors of Dihydroorotate Dehydrogenase. *J. Med. Chem.* **2018**, *61* (12), 5162−5186.
(25) Leelananda, S. P.; Lindert, S. Computational methods in drug discovery. *Beilstein J. Org. Chem.* **2016**, *12*, 2694−2718.
(26) Aprahamian, M. L.; Tikunova, S. B.; Price, M. V.; Cuesta, A. F.; Davis, J. P.; Lindert, S. Successful Identification of Cardiac Troponin Calcium Sensitizers Using a Combination of Virtual Screening and ROC Analysis of Known Troponin C Binders. *J. Chem. Inf. Model.* **2017**, *57* (12), 3056−3069.
(27) Durrant, J. D.; Lindert, S.; McCammon, J. A. AutoGrow 3.0: an improved algorithm for chemically tractable, semi-automated protein inhibitor design. *J. Mol. Graph. Model.* **2013**, *44*, 104−112.
(28) Feixas, F.; Lindert, S.; Sinko, W.; McCammon, J. A. Exploring the role of receptor flexibility in structure-based drug discovery. *Biophys. Chem.* **2014**, *186*, 31−45.
(29) Kim, S. S.; Alves, M. J.; Gygli, P.; Otero, J.; Lindert, S. Identification of Novel Cyclin A2 Binding Site and Nanomolar Inhibitors of Cyclin A2-CDK2 Complex. *Curr. Comput.-Aided Drug Des.* **2021**, *17* (1), 57−68.
(30) Lindert, S.; Zhu, W.; Liu, Y. L.; Pang, R.; Oldfield, E.; McCammon, J. A. Farnesyl diphosphate synthase inhibitors from in silico screening. *Chem. Biol. Drug Des.* **2013**, *81* (6), 742−748.
(31) Lindert, S.; Li, M. X.; Sykes, B. D.; McCammon, J. A. Computer-aided drug discovery approach finds calcium sensitizer of cardiac troponin. *Chem. Biol. Drug Des.* **2015**, *85* (2), 99−106.
(32) Lindert, S.; Tallorin, L.; Nguyen, Q. G.; Burkart, M. D.; McCammon, J. A. In silico screening for Plasmodium falciparum enoyl-ACP reductase inhibitors. *J. Comput.-Aided Mol. Des.* **2015**, *29* (1), 79−87.
(33) Lu, Y.; Vibhute, S.; Li, L.; Okumu, A.; Ratigan, S. C.; Nolan, S.; Papa, J. L.; Mann, C. A.; English, A.; Chen, A.; Seffernick, J. T.; Koci, B.; Duncan, L. R.; Roth, B.; Cummings, J. E.; Slayden, R. A.; Lindert, S.; McElroy, C. A.; Wozniak, D. J.; Yalowich, J.; Mitton-Fry, M. J. Optimization of TopoIV Potency, ADMET Properties, and hERG Inhibition of 5-Amino-1,3-dioxane-Linked Novel Bacterial Topoisomerase Inhibitors: Identification of a Lead with In Vivo Efficacy against MRSA. *J. Med. Chem.* **2021**, *64* (20), 15214−15249.
(34) Hantz, E. R.; Lindert, S. Actives-Based Receptor Selection Strongly Increases the Success Rate in Structure-Based Drug Design and Leads to Identification of 22 Potent Cancer Inhibitors. *J. Chem. Inf. Model.* **2022**, *62* (22), 5675−5687.
(35) Drwal, M. N.; Griffith, R. Combination of ligand- and structure-based methods in virtual screening. *Drug Discov. Today Technol.* **2013**, *10* (3), e395−e401.
(36) Bruno, A.; Costantino, G.; Sartori, L.; Radi, M. The In Silico Drug Discovery Toolbox: Applications in Lead Discovery and Optimization. *Curr. Med. Chem.* **2019**, *26* (21), 3838−3873.
(37) Thirugnanasambantham, P.; Kovvali, S.; Cool, A.; Gao, Y.; Sabag-Daigle, A.; Boulanger, E. F.; Mitton-Fry, M.; Capua, A. D.; Behrman, E. J.; Wysocki, V. H.; Lindert, S.; Ahmer, B. M. M.; Gopalan, V. Serendipitous Discovery of a Competitive Inhibitor of FraB, a Salmonella Deglycase and Drug Target. *Pathogens* **2022**, *11* (10), 1102.
(38) García-Ortegón, M.; Simm, G. N. C.; Tripp, A. J.; Hernández-Lobato, J. M.; Bender, A.; Bacallado, S. DOCKSTRING: Easy Molecular Docking Yields Better Benchmarks for Ligand Design. *J. Chem. Inf. Model.* **2022**, *62* (15), 3486−3502.
(39) Wang, Y.; Wang, X.; Xiong, Y.; Li, C. D.; Xu, Q.; Shen, L.; Chandra Kaushik, A.; Wei, D. Q. An Integrated Pan-Cancer Analysis and Structure-Based Virtual Screening of GPR15. *Int. J. Mol. Sci.* **2019**, *20* (24), 6226.
(40) Ali, A.; Ali, A.; Warsi, M. H.; Rahman, M. A.; Ahsan, M. J.; Azam, F. Toward the Discovery of a Novel Class of Leads for High Altitude Disorders by Virtual Screening and Molecular Dynamics Approaches Targeting Carbonic Anhydrase. *Int. J. Mol. Sci.* **2022**, *23* (9), 5054.
(41) de Sousa, A. C. C.; Combrinck, J. M.; Maepa, K.; Egan, T. J. Virtual screening as a tool to discover new β-haematin inhibitors with activity against malaria parasites. *Sci. Rep.* **2020**, *10* (1), 3374.
(42) Zlotnikov, I. D.; Kudryashova, E. V. Computer simulation of the Receptor-Ligand Interactions of Mannose Receptor CD206 in Comparison with the Lectin Concanavalin A Model. *Biochemistry* **2022**, *87* (1), 54−69.
(43) Carpenter, K. A.; Huang, X. Machine Learning-based Virtual Screening and Its Applications to Alzheimer's Drug Discovery: A Review. *Curr. Pharm. Des.* **2018**, *24* (28), 3347−3358.
(44) Galati, S.; Sainas, S.; Giorgis, M.; Boschi, D.; Lolli, M. L.; Ortore, G.; Poli, G.; Tuccinardi, T. Identification of Human Dihydroorotate Dehydrogenase Inhibitor by a Pharmacophore-Based Virtual Screening Study. *Molecules* **2022**, *27* (12), 3660.
(45) Gokhale, P.; Chauhan, A. P. S.; Arora, A.; Khandekar, N.; Nayarisseri, A.; Singh, S. K. FLT3 inhibitor design using molecular docking based virtual screening for acute myeloid leukemia. *Bioinformation* **2019**, *15* (2), 104−115.
(46) Abohassan, M.; Alshahrani, M.; Alshahrani, M. Y.; Rajagopalan, P. Insilco and Invitro approaches identify novel dual PI3K/AKT pathway inhibitors to control acute myeloid leukemia cell proliferations. *Med. Oncol.* **2022**, *39* (12), 249.

https://doi.org/10.1021/acs.jcim.3c01358
J. Chem. Inf. Model. 2024, 64, 435−448

(47) Kamli, H.; Zaman, G. S.; Shaikh, A.; Mobarki, A. A.; Rajagopalan, P. A Combined Chemical, Computational, and In Vitro Approach Identifies SBL-105 as Novel DHODH Inhibitor in Acute Myeloid Leukemia Cells. *Oncol Res.* **2021**, *28* (9), 899−911.
(48) Zeng, Z.; Konopleva, M. Targeting dihydroorotate dehydrogenase in acute myeloid leukemia. *Haematologica* **2018**, *103*, 1415−1417.
(49) Li, Q.; Shah, S. Structure-Based Virtual Screening. *Methods Mol. Biol.* **2017**, *1558*, 111−124.
(50) Cai, F.; Li, M. X.; Pineda-Sanabria, S. E.; Gelozia, S.; Lindert, S.; West, F.; Sykes, B. D.; Hwang, P. M. Structures reveal details of small molecule binding to cardiac troponin. *J. Mol. Cell. Cardiol.* **2016**, *101*, 134−144.
(51) Berman, H. M.; Westbrook, J.; Feng, Z.; Gilliland, G.; Bhat, T. N.; Weissig, H.; Shindyalov, I. N.; Bourne, P. E. The Protein Data Bank. *Nucleic Acids Res.* **2000**, *28* (1), 235−242.
(52) Madhavi Sastry, G.; Adzhigirey, M.; Day, T.; Annabhimoju, R.; Sherman, W. Protein and ligand preparation: parameters, protocols, and influence on virtual screening enrichments. *J. Comput.-Aided Mol. Des.* **2013**, *27* (3), 221−234.
(53) Shelley, J. C.; Cholleti, A.; Frye, L. L.; Greenwood, J. R.; Timlin, M. R.; Uchimaya, M. Epik: a software program for pK(a) prediction and protonation state generation for drug-like molecules. *J. Comput.-Aided Mol. Des.* **2007**, *21* (12), 681−691.
(54) *Schrödinger Release 2022-3: LigPrep*; Schrödinger: New York, NY, 2021.
(55) Friesner, R. A.; Banks, J. L.; Murphy, R. B.; Halgren, T. A.; Klicic, J. J.; Mainz, D. T.; Repasky, M. P.; Knoll, E. H.; Shelley, M.; Perry, J. K.; Shaw, D. E.; Francis, P.; Shenkin, P. S. Glide: a new approach for rapid, accurate docking and scoring. 1. Method and assessment of docking accuracy. *J. Med. Chem.* **2004**, *47* (7), 1739−1749.
(56) Coldren, W. H.; Tikunova, S. B.; Davis, J. P.; Lindert, S. Discovery of Novel Small-Molecule Calcium Sensitizers for Cardiac Troponin C: A Combined Virtual and Experimental Screening Approach. *J. Chem. Inf. Model.* **2020**, *60* (7), 3648−3661.
(57) Halgren, T. A.; Murphy, R. B.; Friesner, R. A.; Beard, H. S.; Frye, L. L.; Pollard, W. T.; Banks, J. L. Glide: a new approach for rapid, accurate docking and scoring. 2. Enrichment factors in database screening. *J. Med. Chem.* **2004**, *47* (7), 1750−1759.
(58) Harder, E.; Damm, W.; Maple, J.; Wu, C.; Reboul, M.; Xiang, J. Y.; Wang, L.; Lupyan, D.; Dahlgren, M. K.; Knight, J. L.; Kaus, J. W.; Cerutti, D. S.; Krilov, G.; Jorgensen, W. L.; Abel, R.; Friesner, R. A. OPLS3: A Force Field Providing Broad Coverage of Drug-like Small Molecules and Proteins. *J. Chem. Theory Comput.* **2016**, *12* (1), 281−296.
(59) Baell, J. B.; Holloway, G. A. New substructure filters for removal of pan assay interference compounds (PAINS) from screening libraries and for their exclusion in bioassays. *J. Med. Chem.* **2010**, *53* (7), 2719−2740.
(60) Lipinski, C. A.; Lombardo, F.; Dominy, B. W.; Feeney, P. J. Experimental and computational approaches to estimate solubility and permeability in drug discovery and development settings 1PII of original article: S0169-409X(96)00423-1. The article was originally published in Advanced Drug Delivery Reviews 23 (1997) 3−25. 1. *Adv. Drug Deliv. Rev.* **2001**, *46* (1−3), 3−26.
(61) RDKit: Open-Source Cheminformatics. http://www.rdkit.org (accessed Aug 30, 2021).
(62) Deng, X.; Kokkonda, S.; El Mazouni, F.; White, J.; Burrows, J. N.; Kaminsky, W.; Charman, S. A.; Matthews, D.; Rathod, P. K.; Phillips, M. A. Fluorine modulates species selectivity in the triazolopyrimidine class of Plasmodium falciparum dihydroorotate dehydrogenase inhibitors. *J. Med. Chem.* **2014**, *57* (12), 5381−5394.
(63) Bembenek, S. D.; Tounge, B. A.; Reynolds, C. H. Ligand efficiency and fragment-based drug discovery. *Drug Discov. Today* **2009**, *14* (5−6), 278−283.
(64) Kumar, A.; Voet, A.; Zhang, K. Y. Fragment based drug design: from experimental to computational approaches. *Curr. Med. Chem.* **2012**, *19* (30), 5128−5147.
(65) Lyu, J.; Wang, S.; Balius, T. E.; Singh, I.; Levit, A.; Moroz, Y. S.; O'Meara, M. J.; Che, T.; Algaa, E.; Tolmachova, K.; Tolmachev, A. A.; Shoichet, B. K.; Roth, B. L.; Irwin, J. J. Ultra-large library docking for discovering new chemotypes. *Nature* **2019**, *566* (7743), 224−229.
(66) Potlitz, F.; Link, A.; Schulig, L. Advances in the discovery of new chemotypes through ultra-large library docking. *Expert Opin. Drug Discovery* **2023**, *18* (3), 303−313.
(67) Gentile, F.; Yaacoub, J. C.; Gleave, J.; Fernandez, M.; Ton, A. T.; Ban, F.; Stern, A.; Cherkasov, A. Artificial intelligence-enabled virtual screening of ultra-large chemical libraries with deep docking. *Nat. Protoc.* **2022**, *17* (3), 672−697.
(68) Ohio Supercomputer Center. 1987.

https://doi.org/10.1021/acs.jcim.3c01358
J. Chem. Inf. Model. 2024, 64, 435−448